JOURNAL OF GEOPHYSICAL RESEARCH, VOL. 102, NO. C13, PAGES 27,751-27,769, DECEMBER 15, 1997

Seasonal transport variability of the Deep Western Boundary Current in the equatorial Atlantic

Jürgen Fischer and Friedrich A. Schott

Institut für Meereskunde, Kiel, Germany

Abstract. A total of 21 about year-long current meter records in the depth range of the upper and middle North Atlantic Deep Water (NADW) were analyzed to determine the mean and the fluctuations of the upper Deep Western Boundary Current (DWBC) in the equatorial Atlantic. The investigation was based on moored arrays at 44°W from three different deployment periods, 1989/1990, 1990/1991 and 1992/1994, and was supplemented by current profiling along 44°W and 35°W. The approximately 100-km-wide DWBC at 44°W, just north of the equator, was attached to the topography with the current maximum exceeding 70 cm s^{-1}. Currents within the DWBC core followed the topography, and the close agreement between the mean current direction and the direction of maximum variance indicated that the major contribution to the DWBC variability near the equator was due to pulsing rather than meandering. For mean transports of upper and middle NADW, the current meter records were averaged over their deployment duration yielding a best estimate of 13 Sv in the depth range 1000 to 3100 m. The mean transport appeared robust, as subsets of the data from two different years yielded about the same mean transport, namely, 12.4 and 13.6 Sv. The DWBC transport time series showed a definite seasonal cycle, ranging from less than 7 Sv during September/October to about 25 Sv during January/February. Annual and semiannual transport harmonics had similar amplitudes, at about 6 Sv each, and together they explained about two thirds of the total transport variability. After crossing the equator, the DWBC splits into two cores with the major flow along a chain of seamounts near 3.5°S, near 35°W. Magnitudes and phases of the transport variability at 35°W, south of approximately 1.5°S, were similar to that at 44°W. Further, for the flow of lower NADW which was detached from the upper DWBC core, similar periodicity and phases were observed in the deep records at 44°W.

1. Introduction

The Deep Western Boundary Current (DWBC) and its associated transports of North Atlantic Deep Water (NADW) have received increasing attention in the past decade. Current meter records have been analyzed to determine the regional mean DWBC transport and its variability on timescales shorter than a year. Several recent investigations have revealed intraseasonal to interannual variability of the DWBC. Underneath the Gulf Stream near Cape Hatteras, *Pickart and Watts* [1990] showed that besides the presence of energetic topographic Rossby waves at 40-day periods, there were fluctuations of the DWBC associated with the meandering of the Gulf Stream, that is, there was a coupling of the deep transport variability to the upper layer flow.

Paper number 97JC02327.
0148-0227/97/97JC-02327$09.00

In the subtropical Atlantic the longest investigations of the top to bottom western boundary circulation were carried out by *Lee et al.* [1990, 1996] at 26.5°N off Abaco, Bahamas. Intraseasonal variations of the deep transport were dominated by nearly barotropic events of approximately 100-day timescale and appeared to be associated with meandering of the DWBC [*Lee et al.*, 1990]. Superimposed on a mean DWBC transport of 40 Sv (causing speculations about a deep offshore recirculation) were annual and semiannual transport fluctuations of ±13 Sv with southward maxima in October and April/May and minima in summer and winter [*Lee et al.*, 1996]. The authors found these fluctuations to be caused by a barotropic response to remote and local wind forcing at seasonal timescales.

In the tropical Atlantic, off northeastern Brazil, *Johns et al.* [1993] investigated the deeper part of the DWBC which appeared to be separated from the upper core, while farther north near Abaco (26.5°N) only one core exists [*Lee et al.*, 1990, 1996]. The current meter records of a single mooring at 8°N, 52°W (Figure 1) revealed

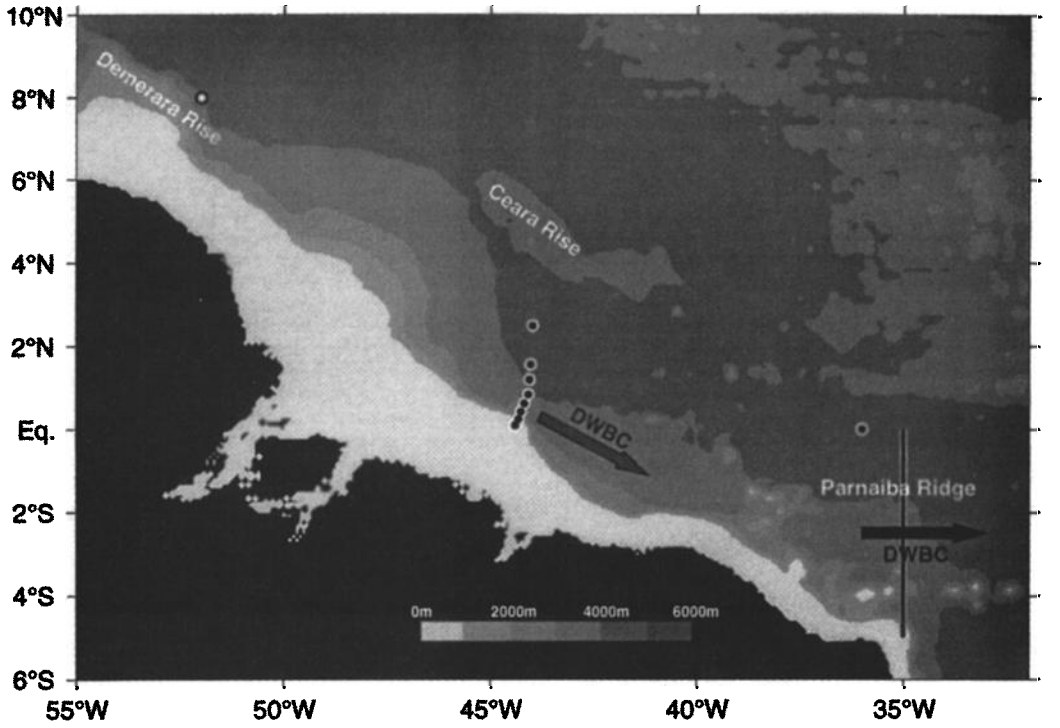

Figure 1. Mooring positions (circles) of the array near 44°W for three deployment periods, 1989/1990, 1990/1991, and 1992/1994; the ship section at 35°W, south of the equator, is included; the 44°W section was parallel to the moored array. Also included are moorings of *Johns et al.* [1993] at 8°N and the equatorial mooring at 36°W. The arrow at 44°W shows the mean current direction of all instruments within the Deep Water core. The bathymetry was taken from the ETOPO5 data set.

an intense DWBC below 2500 m depth with a deep current core at 4300 m [*Johns et al.*, 1993]. In addition to high-frequency variability there was also longer-period variability with remarkably small currents in October/November 1987 (their Figure 6) and a not so pronounced minimum during May 1988, while maxima were found for January to March and July/August. The authors speculated that this variability might be due to thickness variations of the NADW core which then was advected or propagated along the topography. The mean transport of lower NADW was estimated at 22 Sv and agreed well with that determined by *Molinari et al.* [1992] from hydrographic sections between the equator and the Caribbean.

It is only a small fraction of the lower NADW found at the Demerara Rise [*Johns et al.*, 1993] that passes through the 4000-m-deep passage west of Ceara Rise (Figure 1). An isolated current core away from the topography was found south of Ceara at 44°W, 1°30'N in the moored current meter records of *Schott et al.* [1993]. Its mean transport, averaged over the deployment period of approximately 1 year, was estimated to be in the range of 4-5 Sv. However, by comparing the longer-period fluctuations at annual and semiannual timescales with those of *Johns et al.* [1993] from farther upstream, a similar periodicity is apparent. Minimum flow was observed in September–December and again in May, while maxima were found in February/March and June–August. A deep NADW core with similar transport (5 Sv) was found at the Parnaiba Ridge (35°W, 1°30'S; Figure 1) in direct current observations by Pegasus and lowered acoustic Doppler profiler (LADCP) [*Rhein et al.*, 1995]. No further evidence of lower NADW was found along 35°W in the equatorial channel between the shelf and the Mid-Atlantic Ridge, suggesting this being the only cross-equatorial flow of lower NADW in the temperature range 2.2°C to 1.75°C.

The upper and middle NADW seemed to be trapped at the topography [*Molinari et al.*, 1992], and its mean transport at the equator was estimated at 14 to 17 Sv [*Schott et al.*, 1993]. Inspection of their current meter records revealed similar periodicity and phases for the upper and lower core of the DWBC. Although there were discussions about the variability of the DWBC, including annual, semiannual and higher frequencies, an investigation of the upper NADW transport fluctuations was not possible with the limited number of current meter records at that time.

Numerical investigations of the seasonally forced World Ocean Circulation Experiment – Community Modeling

Effort (WOCE – CME) by *Böning and Schott* [1993] revealed variability at different timescales at the NADW depth level (1875 m). The zonal current component at the equator showed seasonal fluctuations which were associated with Rossby waves induced by the seasonally varying wind field over the equator. Near 44°W there were also hints of a semiannual period, although not specifically analyzed in that paper. Higher-frequency fluctuations occurred in the meridional current component at periods near 45 days. These had the characteristics of Rossby - gravity waves (Yanai - waves) and according to *Cox* [1980] are generated by instabilities of the intense upper layer currents and subsequent downward radiation of energy. Other multilevel models also revealed deep variability [e.g., *Philander et al.*, 1986], but at somewhat shorter periods, near 30 days.

The focus of this paper is on the seasonal variability of the Deep Western Boundary Current (DWBC) and its transport fluctuations near the equator. The investigation is based on current meter measurements from three year-long deployments just north of the equator at 44°W and on shipboard current observations from three cruises at 44°W and 35°W. Data from the first and second deployment were already shown by *Schott et al.* [1993] and are complemented by a third deployment period (1992 to 1994) more specifically designed to resolve the upper core of the DWBC. Defined by potential temperature ranges, the upper DWBC core contains upper NADW (Θ=4.5°C – 3.2°C) and middle NADW (Θ=3.2°C – 2.4°C) [*Molinari et al.*, 1992; *Schott et al.*, 1993]. Averaged over all R/V *Meteor* conductivity-temperature-depth (CTD) profiles in the DWBC core, the depth of the selected isotherms was constant within a few tens of meters, and the whole range of upper and middle NADW could equally well be defined by the depth range 1000 – 3100 m.

After a description of the observations, estimates of the mean DWBC transport and transport fluctuations at annual and semiannual timescales will be given, and their causes and consequences will be discussed. Other questions addressed here are; Is there a narrow recirculation at 44°W, as can be detected in general circulation models [*Böning and Schott*, 1993] and by some of the float trajectories of *Richardson and Schmitz* [1993]. What is the fate of the DWBC after crossing the equator? Is there a vertical coupling of the upper layer currents to the DWBC flow?

2. Moored Observations

Three moored arrays have been deployed in the tropical western Atlantic along approximately 44°W just north of the equator. Each array consisted of three moorings; their locations are shown in Figure 1, and their instrument distribution is displayed in Figure 2.

The first array, moorings K327 - K329, was deployed from September 1989 to October 1990, and the second array, moorings K339 - K341, from October 1990 to September 1991. Results from these two deployment periods were presented by *Schott et al.* [1993]. In that paper the focus was on mean and seasonal transports of the upper layer flow and on mean transports associated with the DWBC. The spatial distribution of the moorings for each of the first two deployment periods was not adequate to resolve the DWBC; during both deployments only the near coastal mooring was within

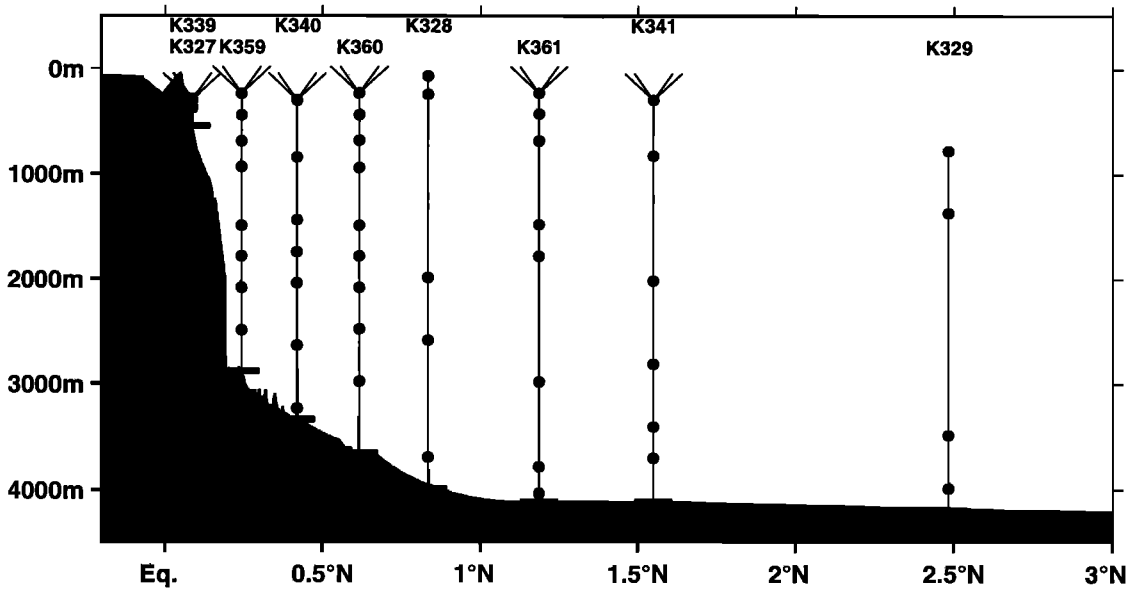

Figure 2. Instrumentation of the current meter array for all three deployment periods; circles represent Aanderaa current meters (RCMs), and circles with upward looking rays symbolize ADCPs; for deployment periods see text. The topography was obtained from the R/V *Meteor* depth sounding system during the deployment cruise in October 1992.

the DWBC, making the horizontal extrapolation somewhat arbitrary. Therefore only a deployment-long mean DWBC - transport was estimated from a combination of all available current measurements in the DWBC. In addition, some transport estimates at extremely low/high DWBC intensities were presented.

The third array, moorings K359-K361, deployed between October 1992 and March 1994, was designed to better resolve the DWBC and to allow the calculation of transport time series. Based on the experience of the earlier deployments, mooring positions were moved closer to the Brazilian shelf with K359 at a water depth of 2880 m (14.6'N), K360 at 3660 m depth (37'N), and K361 at 4110 m depth (1°11.15'N). While the nearshore mooring was always within the core of the DWBC, the offshore mooring was clearly outside. Its position (K361) was chosen to determine the inshore extent of the lower NADW - core centered at 1°30'N and to measure a possible recirculation of the upper NADW [*Schott et al.*, 1993]. The mooring in the center of the array was situated near the offshore edge of the DWBC, being within the DWBC for most of the time. As for the earlier deployments, two types of instruments were used, ADCPs working at 153.6 kHz as top elements near 230 m depth, and Aanderaa rotor current meters (RCMs) everywhere else. Four horizons within the range of the DWBC were occupied, 1500, 1800, 2100, and 2500 m depth (Figure 2, moorings K359 and K360).

Although the deployment duration of that third array was about 16 months, most of the RCM records were short by several months due to power consumption problems of an older generation of vector averaging Aanderaa current meters (type RCM8). However, even the shorter records almost covered 1 year, from October 1992 to October 1993. The temporal resolution originally was 2h, but because we are not interested in subtidal periods here, all records were low-pass filtered (40h cutoff period) and subsampled to 12hours resolution. This data set was complemented by four current meters at upper NADW depth levels, at 1300, 1500, 1700, and 1900 m depth, which were incorporated in an equatorial mooring of M. McCartney (Woods Hole Oceanographic Institution) at 36°W.

Deployment - mean statistics and duration of the records are given in Table 1. The mean current direction was determined by two methods, first from the deployment - mean current components in the core of the DWBC, that is, from 12 records of mooring K359, K360,

Table 1. DWBC Deployment-Long Statistics of Alongshore Flow

Instrument	Record Length	Depth, m	Direction, deg.	Mean, cm s^{-1}	Minimum, cm s^{-1}	Maximum, cm s^{-1}	s.d., cm s^{-1}	Stalled, %
	Mooring K359,		*Oct. 27, 1992 - March 5, 1994, 0° 14.6'N, 44° 18.6'E*					
4	317	936	-74.5	-10.8	34.5	-59.0	24.4	43
6	380	1490	-55.5	-15.9	19.9	-68.7	18.7	0
7	316	1786	-57.0	-39.7	3.4	-74.0	15.2	0
8	417	2085	-62.4	-37.3	5.4	-69.8	15.8	1
9	493	2492	-58.9	-3.3	2.4	-7.9	2.0	8
	Mooring K360,		*Oct. 27, 1992 - March 4, 1994, 0° 37.0'N, 44° 10.0'E*					
4	403	942	-226.1	10.8	35.3	-20.9	11.6	37
5	347	1490	-38.0	-4.5	16.8	-32.0	10.1	3
6	361	1787	-62.8	-18.6	2.5	-39.6	8.8	1
7	491	2084	-73.5	-10.9	2.2	-33.7	6.8	2
8	322	2482	-75.5	-1.5	9.5	-22.9	4.3	20
	Mooring K340,		*Oct. 12, 1990 - Sept. 8, 1991, 0° 25.2'N, 44° 15.0'E*					
3	323	847	-227.4	4.4	39.0	-27.0	16.1	0
4	329	1440	-65.7	-31.3	9.5	-64.7	16.6	0
5	329	1745	-59.0	-22.6	25.7	-68.4	20.9	0
6	330	2042	-57.5	-24.1	6.4	-54.9	11.2	0
7	237	2637	-51.9	-14.1	3.0	-42.4	11.1	1
8	330	3235	-64.0	-3.9	1.6	-16.8	3.2	26
	Mooring K361,		*Oct. 28, 1992 - March 4, 1994, 1° 11.15'N, 44° 2.7'E*					
4	405	1512	92.9	4.1	27.8	-17.2	8.3	4
6	490	2985	173.6	0.4	20.9	-18.2	6.1	4
7	490	3785	-11.5	-4.0	8.7	-23.5	5.9	4
8	490	4035	-18.1	-2.5	7.5	-16.4	3.7	7
	Mooring K328,		*Sept. 5, 1989 - Oct. 11, 1990, 0° 50.0'N, 44° 04.3'E*					
5	399	1990	-52.4	-4.3	6.5	-27.2	5.8	2
6	399	2588	-99.1	-1.3	13.3	-25.1	5.7	3

and K340 (the latter from the period 1990-1991), yielding -60°±9°as the mean direction (see also Table 1), and second from a principle axis deconvolution, that is, determining the direction of maximum DWBC - variance, yielding -64°±6°. A rotation angle of -62°, that is, a counterclockwise rotation with the (negative) DWBC flow toward 118°, was chosen as a compromise between the mean direction of the flow and the direction of maximum variance.

By comparing this direction with the bottom topography in Figure 1 (see arrow at 44°W), it is evident that the DWBC followed the bathymetry upstream of the array. The close agreement between the mean current direction and the direction of maximum variance indicates that the DWBC variability was due to pulsing rather than meandering of the currents across the array. This is important for transport calculations, as will be shown later.

Maximum along-shore currents were around 70 cm s^{-1} and occurred in the 1700-1800 m depth range. In the data from the third deployment the current maximum was in July but confined to mooring K359 closest to the continental slope (Figure 3), forcing this mooring to dive considerably (about 100 m at this level and for about 10 days); at other periods and in the other moorings the vertical excursions were of the order 10-20 m with negligible effects for the following transport calculations. Farther offshore, at K360, where the current had decayed significantly, there was also some evidence for an associated maximum in July (Figure 4). Another period of intense DWBC flow was observed in Janury 1992, this time well observable at both mooring sites. Further, the 2085 m record of K359 showed an intensification of the current in December 1993 similar to that observed a year before, and in both cases following a period of weaker flow in October/November. A similar structure with low DWBC activity in October/November followed by intense flow in January can be seen in the records of mooring K340 (Figure 5) and was already described by *Schott et al.* [1993]. However, it is only in combination with the subsequent time series that this structure suggests a strong annual cycle. In addition, there are indications of semiannual variability, given the secondary current minimum or even reversal in May to June, which is clearly visible in some of the records, for example, the 1490 m record of K359 (1993), the 1490 m and 1787 m records of K360 (1993) and all four DWBC - records of mooring K340 (1991).

At the deepest level in the DWBC, near 2500 m in mooring K359, currents were considerably lower than farther offshore (mooring K340) at the same level measured 2 years earlier (Figures 3, and 5). Since the 2500-m instrument of mooring K359 was rather close to the bottom and to the shelf break, it is likely that a topographic hump upstream of the array, which remained undetected until after the deployment of that mooring, might have had some shadowing effect. However, the mean current direction at that level was not different from that of the DWBC farther out and above, and the low current level could also be an indication of a current decay toward the topography, as has been assumed earlier in the transport estimates of *Schott et al.* [1993].

Farther out, two records in the depth level of the DWBC core showed mean currents in opposite directions, that is, northwestward (Figure 6). The 1483 m

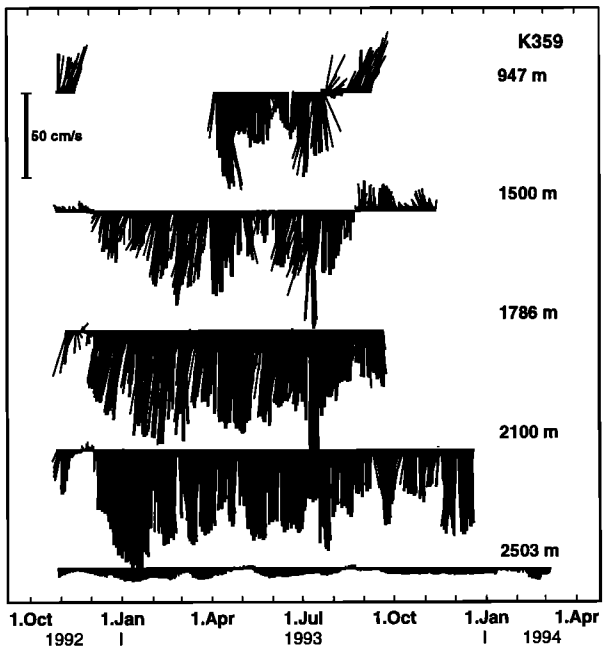

Figure 3. Vector plot of low-pass filtered currents in the upper and middle NADW level near the topography (mooring K359). Currents were rotated counterclockwise (-62°), that is, downward is toward 118°.

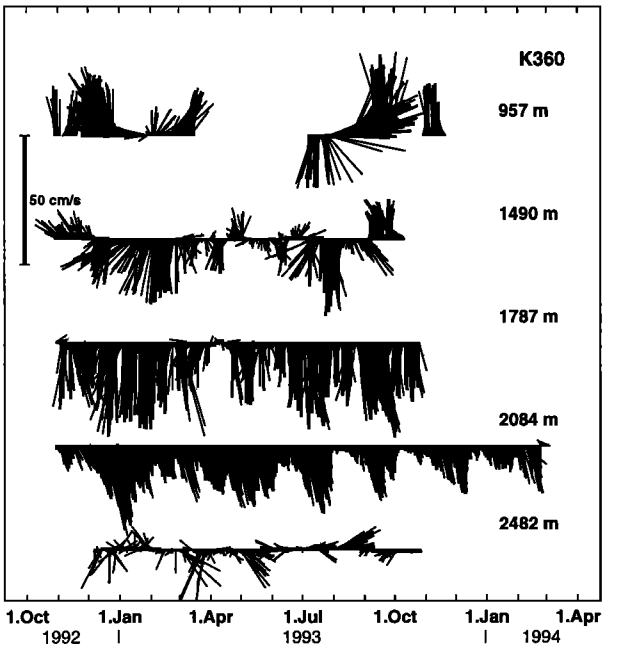

Figure 4. As in Figure 3, but for mooring K360.

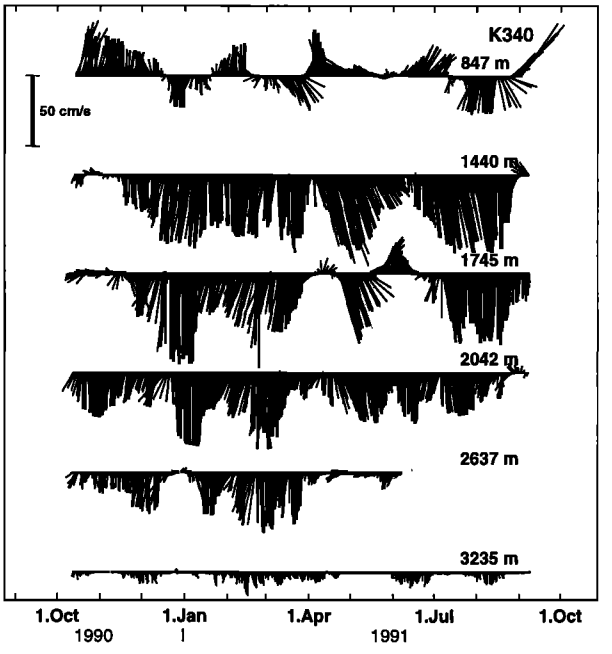

Figure 5. As in Figure 3, but at mooring K340.

deep record of K361 appeared to be within the DWBC at times of intense flow (December to February) and within the recirculation regime at periods of low DWBC activity. About 40 km offshore of K361, the 2020 m deep record of mooring K341 showed more stable northwestward directions, but with large fluctuations at short timescales. Periods of intense recirculation, of more than 20 cm s^{-1}, were observed during January/February and July/August.

An isolated core of lower NADW flow was observed in the 3400 and 3700 m records of mooring K341 (Figure 7). With no further evidence in the earlier records the width of this current core was thought to be similar to that observed upstream by *Johns et al.* [1993]. Mooring K361 of the third deployment, located about 40 km south of K341 (second deployment) contained deep current meters to determine that size more clearly. Consistent with the bathymetry, the mean orientation was more southward at that location, and the currents were somewhat weaker than at K340. Three periods showed current intensification, December 1992, July 1993, and December 1993. In between, the flow was weaker, sometimes even reversing, and indicating the southern edge of the deep current core.

About 900 km east of the array (at 36°W on the equator, Figure 1) the currents in the depth range of upper NADW were dominated by small vertical scales, barely resolved by the current meter separation of 200 m (Figure 8). The major signal was the nearly persistent westward flow at 1500 m depth, averaging to 10.7 cm s^{-1}. Mean eastward currents of 5.1 cm s^{-1} were observed in the deepest of the four records. Besides the high-frequency variability in all levels, there were long

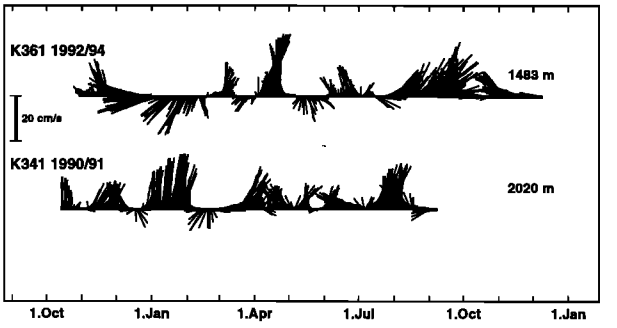

Figure 6. As in Figure 3, but for currents in the recirculation regime at upper NADW levels.

- term trends in the zonal flow, indicative of variability at timescales larger than a year.

3. Shipboard Current Observations

Shipboard observations of deep currents by Pegasus (for the method and errors see *Spain et al.* [1981], and *Send* [1994]) and by LADCP [*Fischer and Visbeck*, 1993] were carried out during R/V *Meteor* cruises M16/3 (May/June 1991), M22/2 (October/November 1992), and M27/3 (March 1994). Subsets of these data have been used in publications describing different aspects of the circulation and watermasses in the western tropical Atlantic [e.g., *Rhein et al.*, 1995; *Schott et al.*, 1993, 1995]. Here the focus is on two meridional sections, at 44°W along the moored array and along 35°W south of the equator.

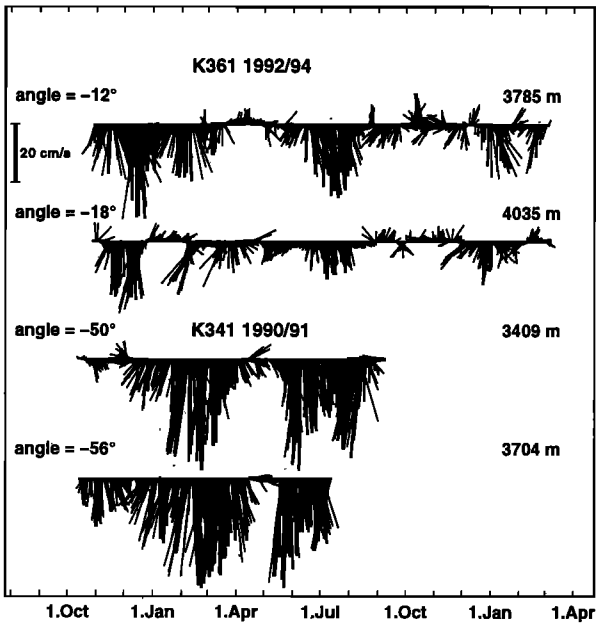

Figure 7. Vector plot of currents at the lower NADW core (moorings K361 and K341). Scaling, rotation angles, and instrument depth as indicated.

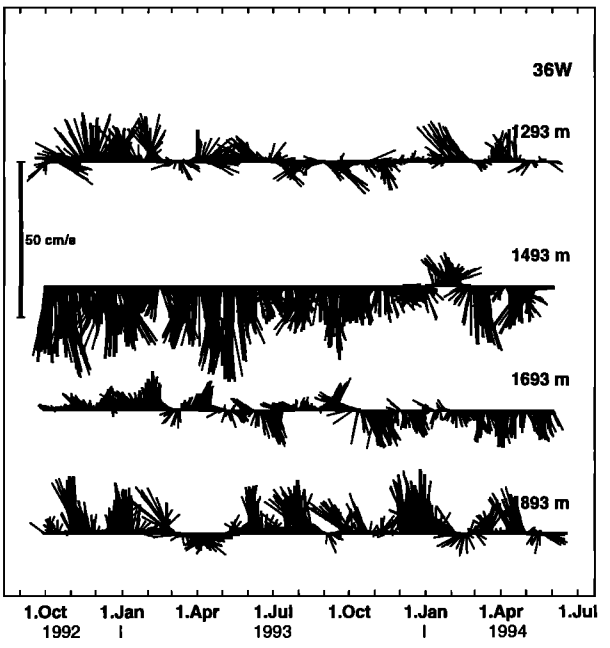

Figure 8. Vector plot of currents at the upper and middle NADW level at the equator, 36°W. Scaling and instrument depth as indicated; downward is to the east.

At 44°W the station spacing of the combined Pegasus/LADCP profiles during the three cruises was adequate to resolve the DWBC. Due to the proximity of the equator, geostrophy could not be applied to determine the currents near the moored array. The deep currents were guided by the topography, such that the DWBC flow (Figure 9) is represented by the alongshore current component alone; negative currents are southeastward (118°) in the direction of the DWBC. For contouring, the currents were smoothed and gridded with a twodimensional Gaussian filter. Cutoff radii of the weighting function were 0.3° in horizontal direction and 50 m in the vertical. All profiles used were down to the bottom, except the one near 0.3°N of M27/3 in the core of the DWBC, which had data only to 2000 m depth. As a result, the flow beyond 2000 m appeared too low, since it was extrapolated from rather weak currents farther north. The structure of the DWBC during M16/3 appeared rather unusual, as there were two cores vertically separated by reverse flow in the depth range 1600 – 2000 m (Figure 9a). This reversal to northwestward direction could also be seen in the 1745 m deep record of mooring K340 (Figure 5). The upper boundary of the DWBC was not so clearly determined as the flow in the DWBC direction extended upward to 800 m, making transport calculations difficult. Within the depth range 1000 – 3100 m and out to 1°N (corresponding to an average DWBC width of 90 km at the 1800 m level [*Richardson and Schmitz*, 1993]) the net transport was 11.6 Sv and somewhat higher (15.4 Sv) when taking only contributions in the direction of the DWBC, that is, without the counterflow. In the other two realizations (Figures 9b and 9c) the core of the DWBC extended from the topography out to 0.8°N followed by recirculation in northwestward direction farther out. It was the vertical scale and the intensity that was different between the M27/3 and M22/2. While in March 1994 (M27/3) the thickness of the core was about 2200 m, it was significantly less during October 1992 (M22/2), at about 1500 m. The thickness variation combined with the variation in the current amplitudes, nearly a factor of 2 at 1800 m depth, explains the large transport difference of 12 Sv (25 Sv during M27/3 and 13 Sv for M22/2). Corresponding to the more intense DWBC in March was the recirculation intensity estimated at 12 Sv for the latitude range 0.7°N to 1.6°N; reducing the net DWBC transport to 13 Sv. Summarizing, combined LADCP and Pegasus profiles from the cruises give an impression of the instantaneous DWBC structure and transports during periods of low intensity (Figures 9a and 9b), and a period of intense DWBC flow (Figure 9c).

At 35°W the same procedure was applied for smoothing and gridding the data, with the horizontal cutoff radii set to 0.4° corresponding to the somewhat larger station spacing. In this area the currents were predominaintly east-west oriented. The zonal current component during the surveys M16/3, M22/2 and M27/3 south of the equator at 35°W showed large variability of the flow at the upper and middle NADW layers (Figure 10, with shaded areas in the direction of the DWBC). In all three surveys there was a small eastward current core hugging the continental shelf break which for M16/3 and M22/2 was mentioned earlier by *Rhein et al.* [1995]. The transport of that core amounted to 1-2 Sv only. It was only partly resolved during M16/3 because of shallow stations near the coast. However, the major eastward current core was found north of a chain of seamounts near 3.5°S (Figure 1), some of which even reach the surface ("Atol das Rocas" and "Arquipelago de Fernando de Noronha"). This core was separated from the coastal core by weaker westward flow. The center of the main core was located between 2°S and 3°S with the most intense flow during M27/3, and considerably lower during M16/3 and M22/2. The total eastward transport between 1.5°S and the coast, depth range 1000 to 3100 m, had a minimum of 6 Sv during early November 1992 (M22/2), a maximum of 20 Sv in mid March 1994 (M27/3), and an intermediate value of 15.5 Sv in early June 1991 (M16/3). The third permanent current feature at 35°W was associated with the deepest component of NADW, the overflow contribution, and was found north of the "Parnaiba Ridge" near 1.5°S. Transports defined between 3500 and 3900 m were 4.5 Sv (October 1990), 6.4 Sv (M16/3, June 1991) and 4.5 Sv (M22/2, early November 1992), as taken from *Rhein et al.* [1995] with a mean of 5.1 Sv. This series was complemented by 9.5 Sv during M27/3 (Figure 10c), leading to a higher mean transport of 6.2±2.4 Sv of lower NADW. At the equa-

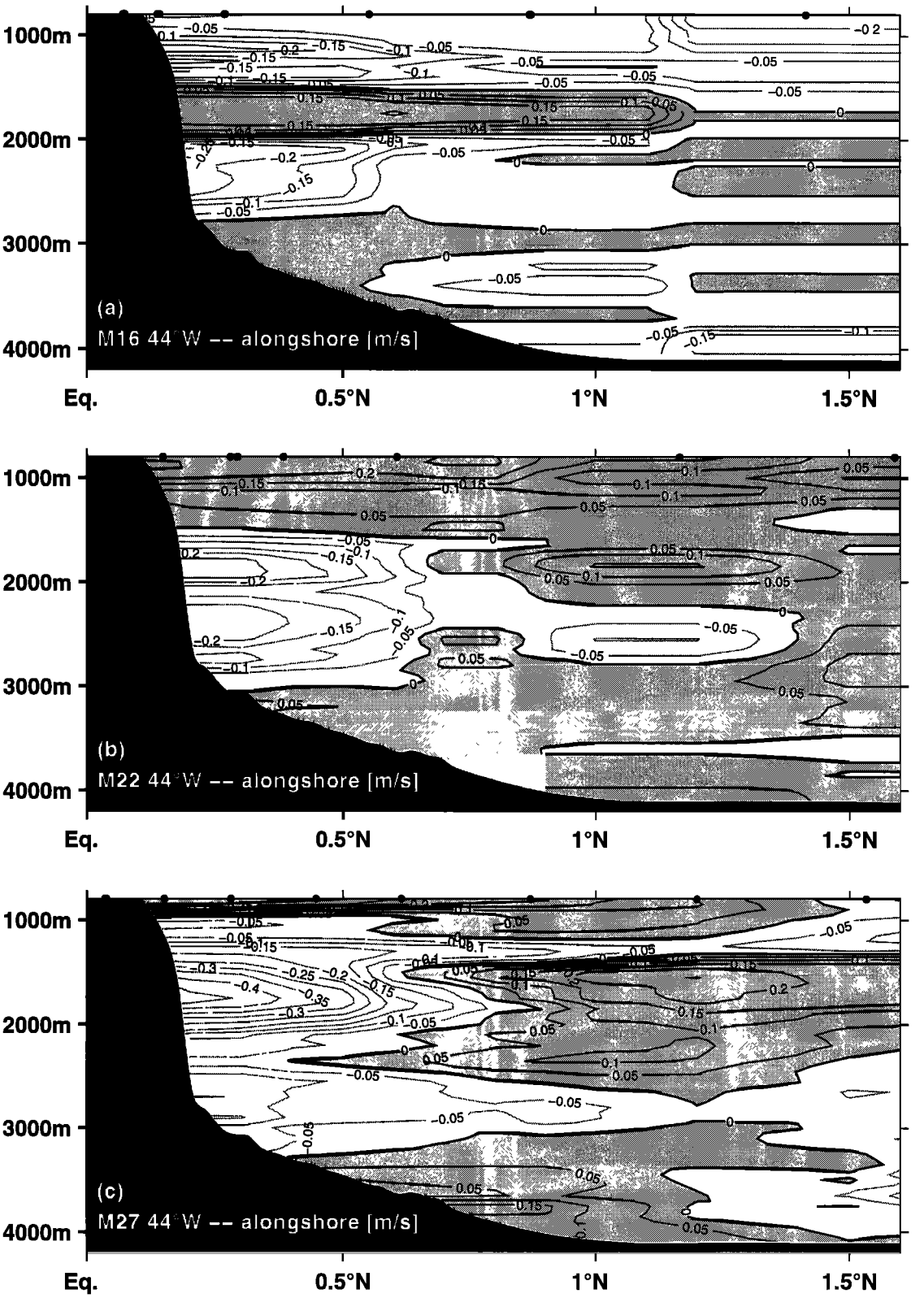

Figure 9. Combined LADCP and Pegasus currents at 44°W in alongshore direction of the DWBC: (a) from *Meteor* cruise M16/3 end of May 1991, (b) from cruise M22/2 end of October 1992, and (c) from cruise M27/3 during early March 1994. The station locations are marked by dots.

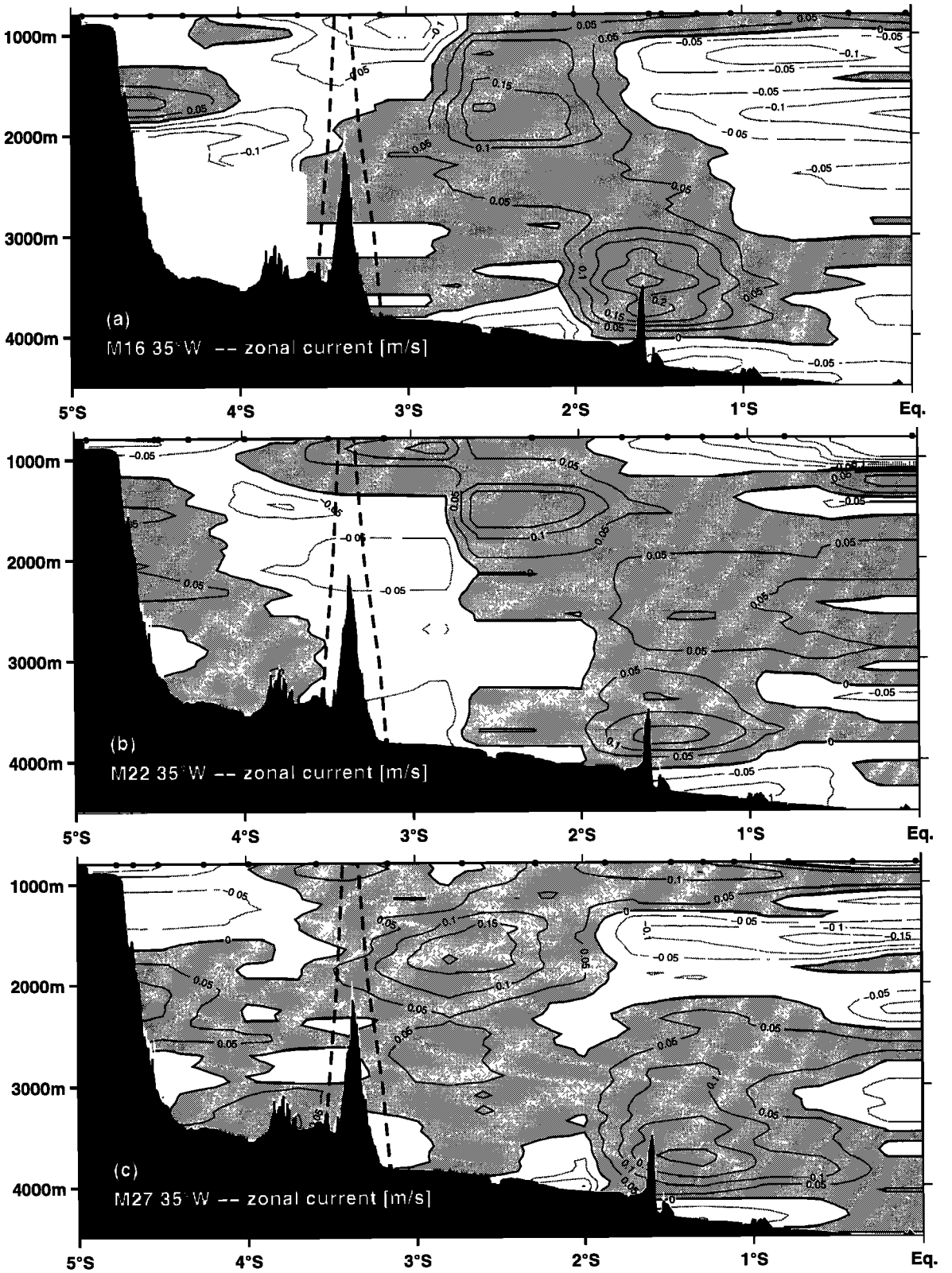

Figure 10. As for Figure 9, but for zonal currents at 35°W sections. The topography just west of the section is indicated by the dashed line.

tor, currents in the upper NADW depth range showed small vertical scales with reversing flow directions (Figure 10) explaining the decorrelation between the equatorial current records at 36°W, which were vertically separated by only 200 m.

4. Mean DWBC Flow and Transport

For the determination of the DWBC - transports a two-dimensional extrapolation scheme is required. In the paper by *Schott et al.* [1993], where only one mooring was within the core of the DWBC, the transports were derived under certain assumptions: the flow should decay linearily toward the topography, and for the offshore side the decay was a linear approximation to the flow field determined by drifter trajectories of *Richardson and Schmitz* [1993]. By this method the record - length mean transport of *Schott et al.* [1993] was 14 Sv compared to an upper limit of 17 Sv obtained with constant extrapolation to the topography. *Johns et al.* [1993] used a two-dimensional Gaussian extrapolation scheme to estimate the mean transport of lower NADW (below 2500 m) off the French Guiana coast, that is, at 8°N, and with the same extrapolation scheme *Schott et al.* [1993] obtained 17.6 Sv.

The data were interpolated to a regular fine resolution mesh of 20 m vertical and 1 km horizontal grid size by objective analysis using a prescribed Gaussian covariance function with length scales of 0.2°horizontally and 400 m vertically. For estimation of the error margins (including measurement errors, insufficient array resolution, and interannual variability) we have averaged the currents from the third deployment (six records from the DWBC core of K359 and K360, 1500 – 2100 m depth) yielding -21.2 cm s^{-1}. We used this value as an estimate for the mean current at the position mooring K340 and calculated the corresponding mean at K340, yielding -26.0 cm s^{-1}. The difference between the two was about 5 cm s^{-1} or 20%.

This was then used for the annual means as a prescibed error margin in the objective mapping resulting in a rms - deviation of 2.9 cm $s^{-1}$of the smoothed field relative to the original data (21 mean current values). Integration of the gridded alongshore flow field yielded a mean transport of 13 Sv for upper and middle NADW (Figure 11) with the uncertainty of the mean estimated at about 2.5 Sv (20%). Variation of the presribed error margins (from 10% to 50%) for the mapping procedure had only a small effect (order 0.5 Sv) on the magnitude of the transport. In comparison to the results *Schott et al.* [1993] based on a subset of the data the mean transport determined here was lower by 1 Sv, which might also be an indication that interannual variability was small.

Using deployment - mean currents from moorings K359, K340, K360, K328, and K361 from a total of 21 current meter records between 800 and 3500 m depth resulted in a rather smooth appearence of the DWBC (Figure 11). Compared to the findings of *Schott et al.* [1993], the addition of the near coastal mooring K359

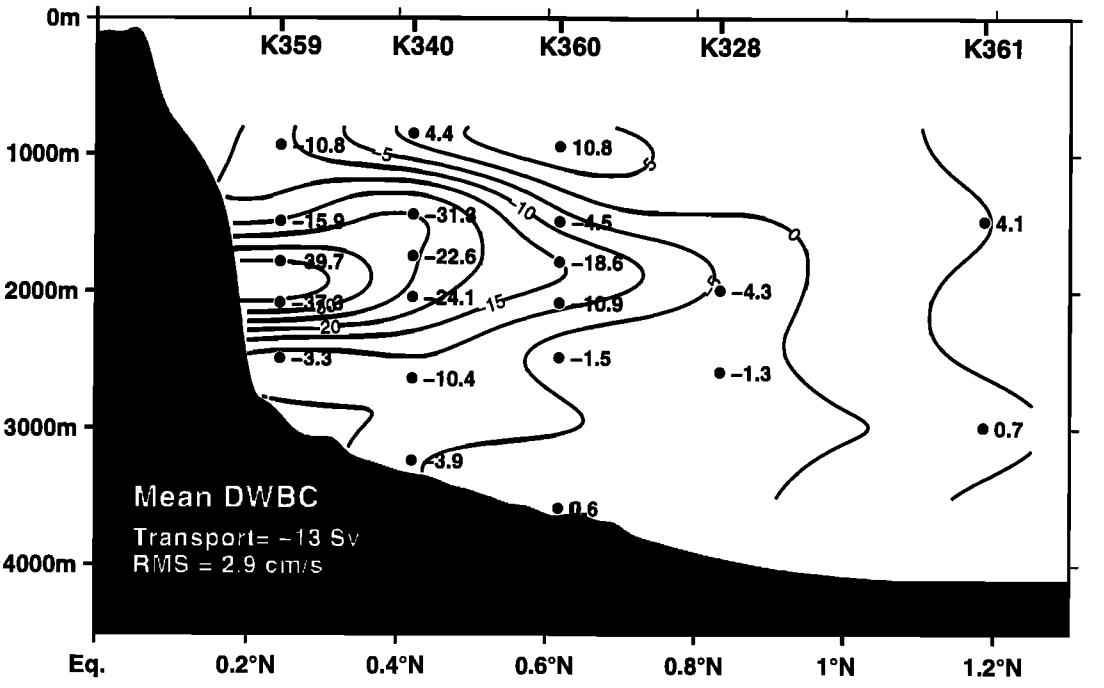

Figure 11. (a) Record length mean DWBC velocities toward 118°. Mooring positions are shown at the top, and instrument positions are marked by dots labeled with the mean current. The contour interval is 5 cm s^{-1}. The mean DWBC transport is defined within the 0 cm s^{-1} isotach. The rms difference of the gridded field relative to the original field is included.

clearly illustrates that the DWBC was not decaying toward the topography. Instead, the DWBC even intensified shoreward from mooring K340 to K359, of which the position of K359 was only 7 km off the 1800 m isobath (Figure 2). Further, the addition of mooring K360 more clearly determined the offshore decay of the DWBC. The width of the DWBC at its core depth determined by the offshore zero - crossing at 1800 m depth was about 90 km, thus confirming the width of the DWBC evaluated from the drifter trajectories by *Richardson and Schmitz* [1993] (see also *Schott et al.* [1993]).

Mean transports from the current meter array and the shipboard observations are summarized in Table 2. Upper NADW defined in the temperature range 3.2°–4.5°C [*Schott et al.*, 1993; *Molinari et al.*, 1992] corresponding to the mean isothermal depth range of 1000 – 2200 m, contributed 9.7 Sv to the DWBC transport. Correspondingly, middle NADW transports below $\Theta = 3.2°C$ and down to the depth of $\Theta = 2.4°C$ (3100 m) were 3.3 Sv. Individual transport estimates from the shipboard measurements revealed large variability, such that an average over only three realizations at each section remains rather uncertain. However, the mean shipboard transports were similar to those determined by the current meter arrays.

5. Variability of the DWBC

5.1. High-Frequency Variability: Spectral Analysis

Inspection of the current time series (Figures 3,4, and 5) shows variability at different periods. Spectral decomposition of the currents rotated to the flow direction of the DWBC was used to determine the variability at timescales shorter than semiannual. Two energetic periods dominate that frequency range, 60-day and 25- to 30-day periods (see also *Schott et al.* [1993]). Besides the higher energy level near the shelf (mooring K359) at all frequencies, it was the 25- to 30-day variability that dominates the shorter-period variance in all three levels of the DWBC (1500, 1800, and 2100 m). There was remarkably little energy at periods below 25 days in the alongshore currents. In this range the energy was concentrated in the cross-flow component with a pronounced peak at 15-day periods.

5.2. Low-Frequency Variability: Harmonic Analysis

Annual and semiannual contributions to alongshore currents in the core of the DWBC (Table 3), comprising moorings K340 (1990/1991), K359 (1992/1993) and three depth levels (1500, 1800, and 2100 m) were determined by harmonic analysis. For comparison, a harmonic analysis was carried out for time series from the recirculation regime (moorings K341 and K361, Figure 6) and for the deep current core near 1.5°N (K341 and K361, Figure 7).

About 50% of the DWBC variance, that was determined by fitting the seasonal harmonics to each of the records individually and subsequently averaging the explained variances (six values), was explained by the combined seasonal harmonics. Because of the rather large harmonic amplitudes, ranging from 5 to 20 cm s^{-1}, it is expected that the DWBC transport variability should show a similar behavior. The annual phase of

Table 2. Mean DWBC Transports for Upper and Middle NADW from Current Meter Arrays and Ship Observations

Transport, Sv	Method	Defined / Range
	Moored Current Meter Array at 44° W	
13.0	objectively mapped mean flow	1000 – 3100 m, DWBC only
9.7	objectively mapped mean flow	$\Theta = 4.5° - 3.2°C$
3.3	objectively mapped mean flow	$\Theta = 3.2° - 2.4°C$
12.4	structure function	1990/1991, 1000 – 3100 m
13.5	structure function	1992/1993, 1000 – 3100 m
13.6	mean of 60-day averages	1000 – 3100 m out to 1.2°N
16.0	mean of 60-day averages	1000 – 3100 m, DWBC only
	Shipboard Measurements at 44° W	
11.6	M16/3	1000 – 3100 m, out to 1.0°N
13.0	M22/2	1000 – 3100 m, out to 1.0°N
25.0	M27/3	1000 – 3100 m, out to 1.0°N
16.5	mean 44°W	1000 – 3100 m, out to 1.0°N
	Shipboard Measurements at 35° W	
15.5	M16/3	1000 – 3100 m, out to 1.5°S
6.0	M22/2	1000 – 3100 m, out to 1.5°S
20.0	M27/3	1000 – 3100 m, out to 1.5°S
13.8	mean 35°W	1000 – 3100 m, out to 1.5°S

Table 3. Harmonics of DWBC Currents and Transports

Mooring/ Period	Depth, m	Annual Amplitude cm s^{-1}	Semiannual Amplitude cm s^{-1}	Annual Phase deg.	Semiannual Phase deg.	Variance Explained %	Rotation, deg.
			Alongshore Currents in Upper DWBC Core				
K359	1500	19.1	8.4	283 (18)	224 (36)	67	-62
K359	1786	19.6	10.6	289 (17)	223 (29)	62	-62
K359	2100	11.9	10.1	260 (29)	224 (33)	49	-62
K340	1440	10.9	12.5	277 (34)	232 (30)	44	-62
K340	1745	8.6	16.5	175 (47)	244 (30)	43	-62
K340	2042	8.2	5.7	232 (33)	175 (44)	31	-62
			Time Series of First EOF - Mode, Upper DWBC Core				
K359/K360		11.0	7.8	274	211	83	-62
			Recirculation in DWBC core level at 44° W				
K361	1483	4.7	4.7	213 (41)	190 (41)	30	-62
K341	2020	1.0	2.6	12 (76)	13(57)	7	-62
			Zonal Currents in DWBC Levels at 36° W, 0° N				
K37W	1293	3.6	1.7	41	333	29	
K37W	1493	1.5	4.4	31	25	18	
K37W	1793	1.6	2.5	303	81	14	
K37W	1993	2.3	2.9	280	7	22	
			Model - DWBC Core at 44° W				
Model		2.0.	1.9	229 (38)	171 (39)	33	-62
			Currents in Lower NADW Depth Range				
K341	3409	—	8.4	—	238 (31)	33	-50
K341	3704	—	8.7	—	265 (28)	36	-56
K361	3785	1.2	6.3	50 (72)	186 (31)	30	-12
K361	4035	8.2	2.7	272 (70)	157 (50)	12	-18
			Upper DWBC - Transports				
1990/1991		4.8*	5.7*	221 (29)	237 (24)	58	-62
1992/1993		6.2*	7.1*	273 (16)	223 (14)	77	-62
			Sverdrup Recirculation Transport				
...	...	5.7*	1.2*	236	287	...	...

*Units in Sverdrups.
Angles in parentheses are for phase errors.

the DWBC core was 247°on average, corresponding to maximum southeastward flow in March, while the semiannual phase was about 220° (maxima in January and July). Phase errors, estimated for assumed 12 degrees of freedom, which is an optimistic estimate, were about 1 month for the annual harmonic and 20 days for the semiannual period.

The similarity of the DWBC phases in the different levels and deployments can be more clearly seen in combined seasonal and semiannual harmonics (Figure 12) with amplitudes scaled for better comparison. The overall maximum in the direction of the DWBC (negative amplitude) was found in December to February, and a secondary maximum in July to August. Minima were found in April to June and September/October. Due to the dominance of the semiannual amplitude at the 1800 m level, the 1990/1991 record appeared somewhat different. However, within the uncertainty of about 1 month the extrema coincided with those of the other records.

Further, harmonic analysis of the time series of the first empirical orthogonal function (EOF) - mode showed that the energy was dominated by annual and semiannual fluctuations explaining 83% of the variance in that mode (Table 3). Including the 60-day period in the harmonic analysis increased the explained variance by only 3%. The other modes had negligible energy concentrated at the higher frequencies.

In the recirculation regime at mooring K361 the harmonics were in phase with the DWBC (Table 3 and Figure 6). This current meter was within the DWBC at times of intense flow and within the recirculation at

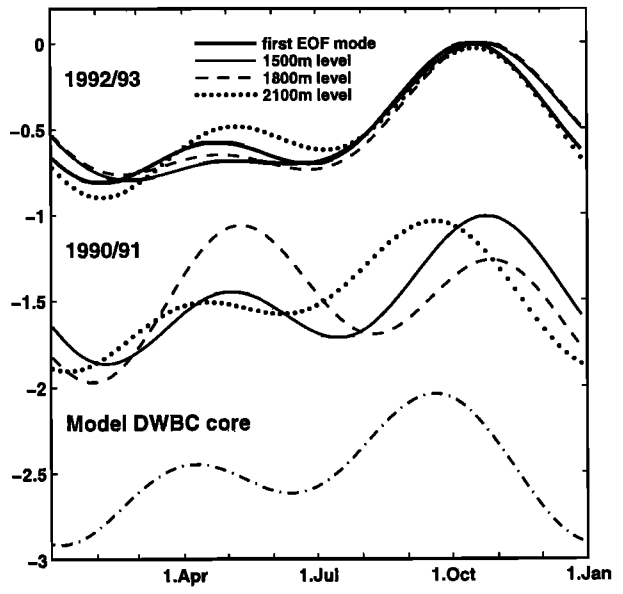

Figure 12. Combined seasonal harmonics of the alongshore flow in the DWBC core, determined from moorings K359 and K340 at levels 1500, 1800, and 2100 m, and for the first mode EOF of the DWBC core (heavy line). Amplitudes are scaled to unity. Bottom curve is for harmonics of the corresponding time series in the general circulation model of A. J. Semtner (personal communication, 1995)

times of low DWBC intensity. At K341, where the currents were mainly flowing northwestward, the variability at annual and semiannual timescales was small (only 7% of the variance was explained by these periods). Phases were subject to larger uncertainties, but there were indications of an 180° phase shift with respect to phases of the DWBC. This points to stronger recirculation when the DWBC was strong, and vice versa.

For the deep core near 1°30'N, associated with the overflow through Denmark Straits (lower NADW), a similar semiannual phase was apparent (Table 3). Although the time series at mooring K341 (1990/1991) were shorter than a year, they clearly revealed weak flow during September to December followed by strong flow during January to March, and again weak currents in April/May. While this was suspected to be coincidental by *Schott et al.* [1993], inspection of the 3800 m deep time series from 1992/1994 (Figure 7, mooring K361) confirmed that it is not. There was clear evidence of current maxima around January and July, and minima in April and October. The simultaneous fit of the harmonics at seasonal periods to the currents rotated to their mean direction explained nearly 30% of the total variance (Table 3). The semiannual phase (212° averaged over the four instruments) was similar to that of the upper DWBC core, while the annual phase (161°) was different by about 2 months (determined only for the third deployment).

6. Transport Variability

The main goal of this investigation was to quantify the transport fluctuations of the DWBC (upper and middle NADW levels) at the equator. For this purpose the alongshore current components at 10-day resolution, as described above, were used. The mean DWBC flow (Figure 11) served as a structure function to relate the currents from the different deployment periods to transport fluctuations on timescales shorter than a year. The hypothesis thereby was that the shape of the DWBC remained unchanged while the current amplitudes might vary, that is, the DWBC pulsed rather than meandered. To test this hypothesis an EOF analysis was performed for the six RCMs of the third deployment period, which were within the core of the DWBC. The calculations were based on time series of 10-day means. The most interesting result was that the first EOF, which had its maximum at the coast and decayed offshore, explained 91% of the total variance. The shape of the first EOF of the DWBC core was similar to the structure of the mean current field (Figure 11). A meandering flow should have considerable variance in modes where the maximum is detached from the topography and there should be a large phase difference between nearshore and offshore records [*Johns and Schott*, 1987]. However, the higher modes together applied for only 9% of the variance, leaving not much energy for a meandering field. As an additional test we compared the ratios of the alongstream variance versus that of the component perpendicular to the DWBC axis. This ratio should be small in a dominantly meandering flow. For the three DWBC - core records of K359 (near the continental slope) the alongstream variance was 35 times the cross-stream variance. Subdividing the records into periods of larger (lower) DWBC intensity, and repeating the calculations yielded a ratio of 21 for periods of intense flow and 10 for weaker than average flow conditions (periods September to November). This is another strong indication for a predominantly pulsing DWBC at 44°W, and if at all, a meandering contribution could only be important during periods of weak DWBC intensity.

For the deployment period October 1992 to October 1993 (K359 and K360) the six current meters within the core of the DWBC were used to determine a scaling factor for the transports during that period. This was done by dividing the 10-day mean currents by the structure function at the instrument positions and subsequently averaging the ratios yielding a time series of scaling factors (at 10-day resolution) with which the mean transport was then multiplied. The same procedure was applied to the four records of mooring K340 for the period October 1990 to September 1991. The basic structure of the two transport time series was very similar (Figure 13) with low transports in the periods September-November and May-June, and larger than average transports in January-March and around

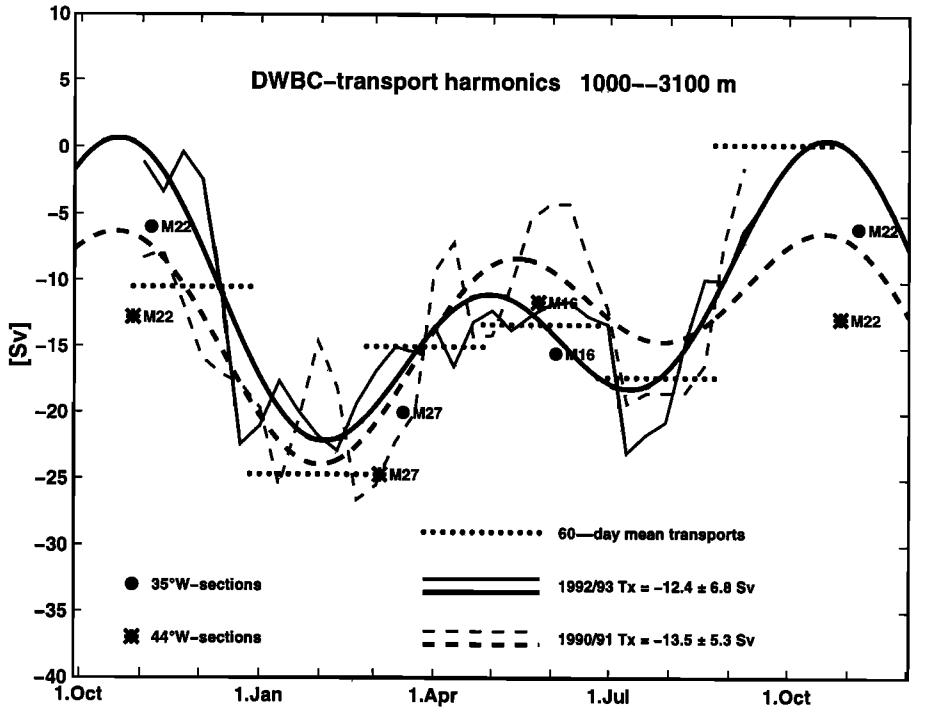

Figure 13. Ten-day mean DWBC transports for deployment periods 1992/1993 and 1990/1991 (thin lines). Combined annual and semiannual harmonics (heavy lines with corresponding signatures). Annual mean and standard deviation of the transport harmonics are shown at bottom. Transports from shipboard profiling sections with LADCP/Pegasus are shown as stars for the 44°W section and as circles for the 35°W section. Transports from 60-day averaged current meter records are shown as dotted lines.

July. Maximum transports determined were between 23 and 27 Sv during January to March, while in September/October the DWBC nearly vanishes. Both time series had about the same mean transport of 13 Sv, as is expected for a structure function that is representative for the appearence of the DWBC at any time. However, due to the shortness of the two time series the annual mean might be a little smaller. Apparently, October, which was partially missed in both records, should have low transports. This was supported by extending the time series from 1992/1993 into that period by the available records (see Figures 3, and 4). Then the annual mean transport was 12 Sv, that is, 1 Sv lower than the average of the time series in Figure 11.

For both deployments the seasonal transport harmonics explained a large part of the transport variability, 58% of the variance in the period 1990/1991 and 77% for the period 1992/1993 (Figure 13 and Table 3). Annual and semiannual fluctuations were about equally important, with amplitudes between 4.8 and 7.1 Sv (Table 3). With respect to phases, there was close correspondence between the two deployment periods for the semiannual oscillations. The annual harmonics were shifted by about 50 days between the deployments, but due to the shortness of the time series the uncertainty of the fit was of similar magnitude (Table 3). Annual mean transports based on the harmonics yielded 12.4 and 13.5 Sv, respectively. For comparison, the instantaneous section transports, evaluated from shipboard profiling at 44°W and 35°W are included in Figure 13, showing satisfactory agreement.

The second approach was to determine the annual and semiannual transport variability by treating the currents from the different deployment periods as if they were from the same seasonal cycle. It has been shown that the semiannual variability from the two different deployment periods was phase locked to the season. Further, the transports determined by the structure function method showed not much interannual variability. By averaging over 60-day intervals the contribution of the high-frequency fluctuations (25-day and 60-day periods) were significantly reduced. Then the 60-day mean currents were interpolated onto a fine-resolution grid by the same procedure as applied to the mean field (Figure 14). Different from the above procedure, the structure of the DWBC was not fixed to the deployment mean, thus a thickness variation of the DWBC would be included.

Even in intervals of rather weak flow the core of the DWBC was near 2000 m depth. Taking the 5 cm s^{-1} contour as the outer edge of the DWBC, the width of the DWBC changes by about 20 km depending on the

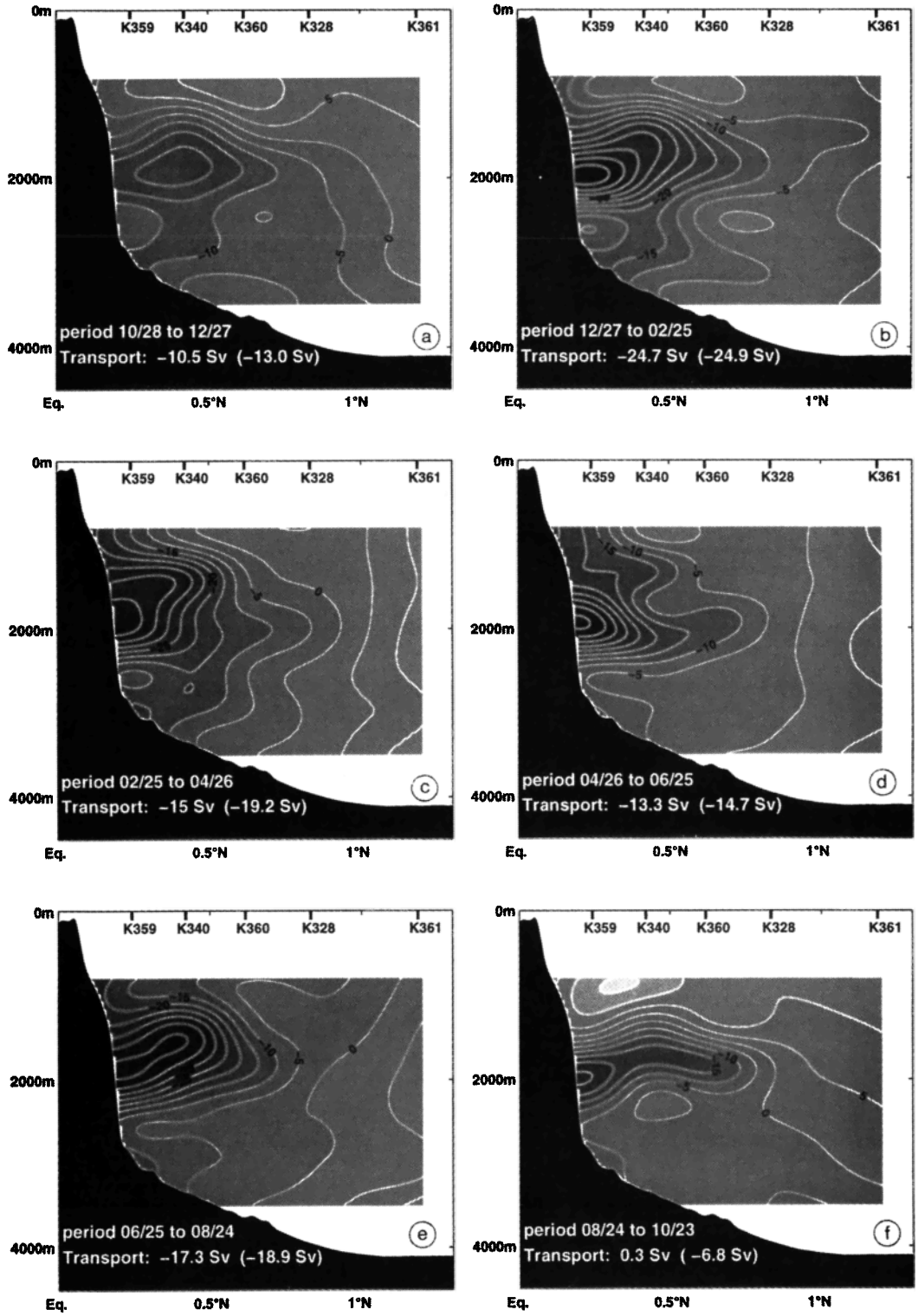

Figure 14. Sixty-day mean DWBC flow patterns from combined measurements of the three deployment periods. Mooring positions are shown at the top of each map. The contour interval is 5 cm s^{-1}. Net transports in the depth range 1000 m – 3100 m and out to 1.2°N are shown at bottom; contributions in the DWBC flow direction in parentheses.

intensity of the flow. The largest offshore extent of the DWBC is observed in January/February, with the 5 cm s^{-1} isotach reaching the position of mooring K361 at about 1°11'N.

There were also changes in the thickness of the DWBC; at times it extended vertically to 3200 m, for example, in January/February, while in other periods the lower boundary was found near 2600 m depth (see also Figure 9). The upper DWBC limit was not so well defined, because the near shre instrument at 936 m depth had temporary data drop outs, as during January/February 1993. In periods of low DWBC intensity (Figures 14a, and 14f) the flow above 1500 m was in opposite direction, and the DWBC appeared as a thin lense in the 1500 – 2100 m depth range. The total range of the DWBC transports (determined by this method), between 1000 and 3100 m depth, ranged from 0 to 25 Sv with a mean of 13.4±8.2 Sv. These values were in reasonable agreement with those obtained by the structure function method (see dotted lines in Figure 13). By taking only the contributions in the direction of the DWBC the mean was somewhat higher, at 16±7 Sv. Most of the difference was from periods of low DWBC intensity, as there was significant northwestward flow near the upper and lower boundaries of the integration during these periods.

7. Summary and Discussion

7.1. Summary of Results

A total of 21 about year-long current meter records in the depth range of the upper and middle NADW (above 3100 m depth) were analyzed to determine the mean and the fluctuations of the upper DWBC in the western equatorial Atlantic at 44°W. The annual mean DWBC transport from two different deployment periods was about 13 Sv. Fluctuations at annual, semiannual and shorter timescales were large, varying from less than 7 to 25 Sv. A harmonic analysis for two different deployments (1990/1991 and 1992/1993) shows that annual and semiannual fluctuations contributed about the same, about 6 Sv each, with nearly identical phases between the years. Extending the harmonic analysis by including the 60-day fluctuations yields a contribution of 1-2 Sv for that period. However, in the harmonic analysis of the first EOF mode the inclusion of the sixth harmonic led to only 3% increase in explained variance, indicating that 60-day variability was not phase locked to seasonal variability. Shipboard transport estimates (Table 2) at 44°W were within the range of estimates from the current meter arrays, but at this large variability and only three realizations the mean transport from the shipboard observations was rather uncertain. Similarly, the mean 35°W transport (Table 2) should be treated with great care.

The first EOF showed the current maximum attached to the topography, and most of the current variability for timescales longer than 10 days was concentrated in the first EOF, with 91% of the total variance explained. Further, equal directions of maximum flow variance and mean flow, and the dominance of along-flow variance compared to cross-flow variance, led to the conclusion that most of the DWBC variability at 44°W was due to pulsing and not to meandering along the topography. This contrasts with the findings for the lower DWBC core farther upstream at 8°N, for which *Johns et al.* [1993] found meandering to be important. As a consequence of the pulsation at 44°W, the mean DWBC flow pattern, here the upper and middle NADW layers, could be treated as a structure function for the transport fluctuations on annual and semiannual timescales. The only indication of a meandering contribution is the weak offshore flow maximum during November – December in Figure 14a.

No significant interannual variability could be detected. Mean transports from subsets measured in different years differed by only 1–3 Sv, and a similar range of transports was obtained by different transport calculation methods applied to the full data set. Further, annual and semiannual transport harmonics for different years differed by 25%–30% (Table 3), that is, by 1–2 Sv, and are not distinguishable within the error bounds.

In comparison with the mean geostrophic estimates of *Molinari et al.* [1992] the mean transport of NADW in the depth range 1000 – 3100 m (corresponding to the range of potential temperatures from 4.5°C to 2.4°C [see *Schott et al.*, 1993]), our values were about 2 – 3 Sv higher. However, their August 1989 transport at 44°W was 15.5 Sv, similar to the August values presented here (Figure 13). Their lower mean transports might therefore be caused by seasonal biasing, as the majority of their measurements were from periods of low DWBC activity (September).

7.2. Comparison of the Upper DWBC With SOFAR - Float Trajectories

The horizontal structure of the upper DWBC at 44°W at 1800 m depth is compared in Figure 15 with the DWBC structure evaluated from SOFAR floats [*Richardson and Schmitz*, 1993]. Bearing in mind that the latter was composed from float trajectories along the entire western boundary of the northern tropical Atlantic between 7°N and the equator, the offshore decay and the width (90 – 100 km) of the DWBC at 44°W is surprisingly similar. Further, there are indications both in the moored and float data of a stable recirculation offshore of the zero crossing of the flow. However, the range over which the DWBC varied (according to our study) at seasonal periods was large (Figure 15), especially near the topography where the current maximum was observed. This was also the area with the largest deviations between the two data sets; while the float data strongly decayed toward the topography, the cur-

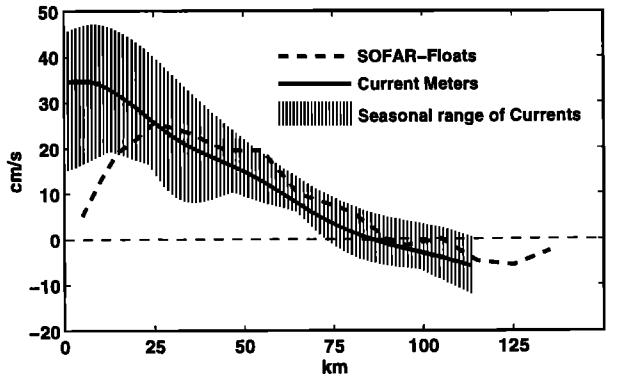

Figure 15. The DWBC in the western tropical Atlantic at 1800 m depth versus offshore distance from the 1800-m isobath. Heavy dashed line represents the mean DWBC as deduced by SOFAR float trajectories (redrawn from *Richardson and Schmitz* [1993]). Heavy solid line shows the mean flow averaged over the six realizations shown in Figure 14 for the 1800-m level, and the shaded area indicates the range spanned by the six realizations.

rent meter data at 44°W had the maximum closest to the topography. This is not artificially generated by the objective mapping but is confirmed by the current measurements at 1786 m depth, mooring K359, which was located less than 7 km away from the 1800 m isobath (Figure 2). There are several possible reasons for this difference, which include different slopes of the continental shelf break between 44°W and other regions of the tropical Atlantic where the float measurements were taken, uncertainties in the depth of the floats, and aliasing by temporal variability. The mean transport estimate of *Richardson and Schmitz* [1993] was 15 Sv based on the float trajectories and a vertical structure determined from a single mooring at 6.2°N, 51°W [*Colin et al.*, 1991], which is similar to the 13 Sv determined in this study at 44°W.

Richardson and Schmitz [1993] divided their float records into three periods of nearly equal data density and obtained the most intense flow near the boundary for the period January to October 1989, followed by somewhat weaker currents between November 1989 to April 1990, and weakest between May to October 1990. Maximum DWBC speeds were observed from floats launched in January and February 1989. Although *Richardson and Schmitz* [1993, page 8376] mentioned that conclusions about time variability were somewhat subjective, they noticed "that speeds and transports decreased monotonically over the three subsets, suggesting low frequency variability." The seasonal variability determined here from the moored array indicated that the high float velocities during January to March 1989 were due to the combined annual and semiannual DWBC maxima in that period rather than due to longer-period variability.

7.3. Recirculation of the DWBC at 44°W

Evidence of a narrow DWBC recirculation was found in the float trajectories of *Richardson and Schmitz* [1993] and was estimated at 6 Sv based on a vertical current profile by *Colin et al.* [1991]. In the float trajectories the recirculation appeared rather intense in the 100 km adjacent to the DWBC and more variable farther out. Evidence of a narrow recirculation cell at 44°W, amounting to 12 Sv, was also obtained by the ship section M27/3 during the height of the DWBC (Figure 9c) thereby reducing the net southeastward transport to about the annual mean across the extent of the section covered. The high freon content of the uppermost NADW constituent during that survey was found to extend to the north of the DWBC (M. Rhein, personal communication, 1996) supporting the idea of a narrow recirculation cell adjacent to the DWBC at 44°W, rather than showing reverse flow of water masses from a different origin.

In the CME model analyzed by *Böning and Schott* [1993] and in the global model of *Semtner and Chervin* [1992], narrow eddy-like recirculation cells exist along the DWBC path in the tropical Atlantic and especially near 44°W. Fluctuations in the model recirculation [*Semtner and Chervin*, 1992] are correlated with fluctuations of the DWBC, similar to what is seen in the 2020-m-deep record at mooring K341.

From the available evidence it is risky to estimate the recirculation transport and whether it has a seasonal cycle as does the DWBC. What is now the total deep flow into the equatorial regime from the north? From shipboard observations [*Rhein et al.*, 1995] and moored current meter records [*Schott et al.*, 1993] there is evidence of about 5–6 Sv lower NADW approaching the equator between 44°W and 35°W. The equatorial channel at 35°W was well covered by direct current observations making it unlikely that additional flow of lower NADW remained undetected. In combination with the mean transport (13 Sv) of the upper and middle NADW the inflow into the equatorial regime amounts to 19 Sv without taking recirculation transports into account, that is, this value represents an upper limit for the interhemispheric NADW transfer. This is fairly close to other estimates of the "conveyor belt" overturning circulation in the Atlantic [e.g., *Roemmich and Wunsch*, 1985; *Schmitz*, 1995], meaning that the net deep recirculation at 44°W should be small.

7.4. Upper DWBC South of the Equator

The path of the upper DWBC after crossing the equator is strongly influenced by the complicated topography, as is illustrated by the float trajectories of *Richardson and Schmitz* [1993]. At 35°W, taht is, about 1000 km downstream of the moored array, two cores of upper NADW were observed (Figure 10), a weak core attached to the coast and the main flow farther out between 3°10'S and 1°50'S separated by more variable flow in between (see also *Rhein et al.* [1995]).

In all three surveys the transport of the core at the shelf break, across 35°W, amounted to 1-2 Sv only, indicating that the main DWBC flow occurred along the offshore edge of a chain of seamounts near 3.5°S (Figure 1). This path of the DWBC is also supported by an individual 1800-m float trajectory of *Richardson and Schmitz* [1993]. It could further be speculated that the small core attached to the coast might be due to leakage through the gaps of the seamount chain farther upstream.

The eastward transport between of 1.5°S and the coast, depth range 1000 to 3100 m, increased from 6 Sv during early November (M22/2) to 20 Sv in mid March (M27/3) followed by a decrease to 15.5 Sv in early June (dots in Figure 13) reflecting a transport variability similar to that observed at 44°W. Transports of the lower NADW core north of the Parnaiba ridge, 1.5°S, varied by a factor of 2 depending on the time of the measurements. They show a similar cycle as the upper DWBC core, and consequently the mean transport from the three *Meteor* surveys could be biased toward low values by about 1 Sv. A deep annual cycle is also supported by the current meter time series near 1°20'S, 36°W by *Hall et al.* [1997], which varied roughly in phase with our observations.

7.5. Annual and Semiannual Variability in High-Resolution Models

We used the monthly mean output of the eddy-resolving global ocean circulation model of *Semtner and Chervin* [1992] forced by monthly wind stress for comparison with the observations. The model DWBC at 44°W appeared to be separated from the boundary, with the core of the DWBC at 0.6°N decaying toward the topography and northward, while the observed DWBC was hugging the continental slope. Observed DWBC currents were about 2 to 3 times stronger than in the model realization. Also different were the horizontal and vertical structure of the model DWBC, which appeared as a single jet extending out to 2°N and from about 1000 m down to more than 4000 m. However, a harmonic analysis of the currents averaged over the two near coastal grid points (0.2°N and 0.6°N) and the depths layers 1542, 1975, and 2475 m,that is, the core of the DWBC, revealed phases similar to the observations (Figure 12, and Table 3). The absolute minimum intensity of the model was in September, about 1 month earlier than indicated by most of the current measurements but almost identical with the observations in the 2100-m level of the second deployment (1990/91). Model amplitudes of the annual and semiannual harmonics were nearly the same for the averaged currents, at 2.0 and 1.9 cm s^{-1}, respectively, that is, much smaller than the mean of about 9 cm s^{-1}. In the observations the ratio between the harmonic amplitudes versus the mean scaled like one half to one third.

As regards a possible origin of seasonal DWBC variability, *Böning and Schott* [1993], in their analysis of the CME model, showed it to be linked to Rossby waves induced by the seasonally varying wind field over the equator. The seasonality in the NADW layer ceased, when the seasonal forcing was switched off and the model was forced by constant winds.

7.6. Comparison to Sverdrup Recirculation

The transport required to balance the interior Sverdrup circulation [see *Schott et al.*, 1993] has an annual range of about 15 Sv with a minimum in March and a maximum in August to September. Harmonic decomposition into annual and semiannual contributions shows that the Sverdrup recirculation has an annual harmonic at the equator, which is in phase with that of the DWBC (Table 3, and Figure 16). Further, the associated annual harmonic transport was 5.7 Sv, similar to the two estimates obtained for the DWBC (4.8 and 6.2 Sv). For a complete comparison one would have to add the contributions of the upper layer flow, as well as contributions of the lower NADW layers from outside our arrays. However, in the presence of very energetic higher-frequency fluctuations [*Schott et al.*, 1993] a consistent annual and semiannual cycle of the North Brazil Current at 44°W could not be determined from the different array repeats, and for the lower NADW layer spatial and seasonal coverage was not sufficient. Comparing the semiannual components, the contribution of the Sverdrup recirculation is rather weak compared to the DWBC variability and shows a phase shift of about 1 or 2 months relative to the semiannual phase of the DWBC (Figure 16).

Summarizing, the similarity of the annual phases suggests a response of the boundary current regime to the interior Sverdrup forcing, as has been found in other regional investigations [e.g., *Lee et al.*, 1996]. In that study the authors found both annual and semiannual

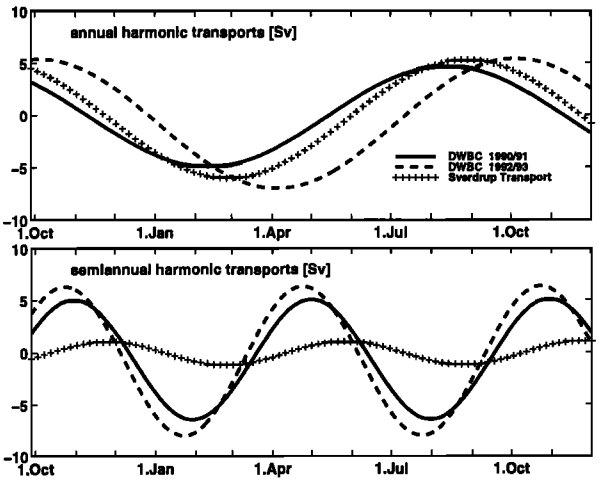

Figure 16. (top) Annual harmonic transports of the DWBC and of the Sverdrup recirculation determined by *Schott et al.* [1993]. (bottom) Semiannual harmonic transports.

transport fluctuations of the DWBC in agreement with the corresponding Sverdrup recirculation. Here the semiannual component of the Sverdrup recirculation appeared too weak to explain the observed deep variability as a direct response to semiannual wind forcing. Another possible mechanism for generating the observed semiannual variability could be interaction of equatorial waves, that are not caused by the Sverdrup forcing, with the slanting western boundary.

Acknowledgments. We thank captains and crews of R/V *Meteor* for their friendly and competent help with mooring deployments and retrievals. We wish to thank J. Reppin for helping with the current meter processing and many helpful discussions, and U. Send and G. Krahmann for their help with the Pegasus data. We are grateful to C. Colin, who loaned us four current meters for the 44°W array. We would also like to thank M. McCartney for allowing us to put our current meters into his equatorial mooring at 36°W. Finally, we would like to thank A. J. Semtner for making his model data available to us. This work was funded by the Deutsche Forschungsgemeinschaft (DFG), Sonderforschungsbereich 133, and grants Scho 168/21-1, Scho 168/21-2, and by the Bundesministerium für Forschung und Technologie (BMFT), grant 03F0121A. The R/V *Meteor* cruises were also supported by Deutsche Forschungsgemeinschaft.

References

Böning, C. W., and F. Schott, Deep currents and the eastward salinity tongue in the equatorial Atlantic: Results from an eddy-resolving, primitive equation model, *J. Geophys. Res.*, *98*, 6991–6999, 1993.

Colin, C., J. M. Bore, R. Chuchla, and D. Corre, Programme NOE, Resultats de courantometrie (mouillage de subsurface) au point 6°12'N–51°01'W du 31 mars au 18 novembre 1990, *Doc. Sci., Cent. ORSTOM de Cayenne, Cayenne, French Guiana*, *4*, 1991.

Cox, M. D., Generation and propagation of 30-day waves in a numerical model of the Pacific, *J. Phys. Oceanogr.*, *10*, 1168–1186, 1980.

Fischer, J., and M. Visbeck, Deep velocity profiling with self-contained ADCPs, *J. Atmos. Oceanic Technol.*, *10*, 764–773, 1993.

Hall, M. M., M. S. McCartney, and J. A. Whitehead, Antarctic bottom water flux in the equatorial western Atlantic, *J. Phys. Oceanogr., in press*, 1997.

Johns, W. E., and F. Schott, Meandering and transport variations of the Florida Current, *J. Phys. Oceanogr.*, *17*, 1128–1147, 1987.

Johns, W. E., D. M. Fratantoni, and R. J. Zantopp, Deep western boundary current variability off northeastern Brazil, *Deep Sea Res.*, *40*, 293–310, 1993.

Lee, T. N., W. Johns, F. Schott, and R. J. Zantopp, Western boundary current structure and variability east of Abaco, Bahamas at 26.5°N, *J. Phys. Oceanogr.*, *20*, 446–466, 1990.

Lee, T. N., W. E. Johns, R. J. Zantopp, and E. R. Fillenbaum, Moored observations of western boundary current variability and Thermohaline circulation at 26.5°N in the subtropical North Atlantic, *J. Phys. Oceanogr.*, *26*, 962–983, 1996.

Molinari, R. L., R. A. Fine, and E. Johns, The deep western boundary current in the western tropical North Atlantic Ocean, *Deep Sea Res.*, *39*, 1967–1984, 1992.

Philander, S. G. H., W. J. Hurlin, and R. C. Pacanowski, Properties of long equatorial waves in models of the seasonal cycle in the tropical Atlantic and Pacific oceans, *J. Geophys. Res.*, *91*, 14207–14211, 1986.

Pickart, R. S., and D. R. Watts, Deep western boundary current variability at Cape Hatteras, *J. Mar. Res.*, *48*, 765–791, 1990.

Rhein, M., L. Stramma, and U. Send, The Atlantic deep western boundary current: Water masses and transports near the equator, *J. Geophys. Res.*, *100*, 2441–2457, 1995.

Richardson, P. L., and W. J. Schmitz, Deep cross-equatorial flow in the Atlantic measured with SOFAR floats, *J. Geophys. Res.*, *98*, 8371–8387, 1993.

Roemmich, D. H., and C. Wunsch, Two transatlantic sections: Meridional circulation and heat flux in the subtropical North Atlantic Ocean, *Deep Sea Res.*, *32*, 619–664, 1985.

Schmitz, W. J. J., On the interbasis-scale thermohaline circulation, *Rev. Geophys.*, *33*, 151–173, 1995.

Schott, F., J. Fischer, J. Reppin, and U. Send, On mean and seasonal currents and transports at the western boundary of the equatorial Atlantic, *J. Geophys. Res.*, *98*, 14353–14368, 1993.

Schott, F., L. Stramma, and J. Fischer, The warm water inflow into the western tropical Atlantic boundary regime, spring 1994, *J. Geophys. Res.*, *100*, 24745–24760, 1995.

Semtner, A. J., and R. M. Chervin, Ocean general circulation from a global eddy-resolving model, *J. Geophys. Res.*, *97*, 5493–5550, 1992.

Send, U., The accuracy of current profile measurements: Effect of tropical and mid latitude internal waves, *J. Geophys. Res.*, *99*, 16229–16236, 1994.

Spain, P. F., D. L. Dorson, and H. T. Rossby, PEGASUS: A simple acoustically tracked velocity profiler, *Deep Sea Res.*, *28*, 1553–1567, 1981.

J. Fischer and F. A. Schott, Institut für Meereskunde an der Universität Kiel, Düsternbrooker Weg 20, 24105 Kiel, Germany. (e-mail: jfischer@ifm.uni-kiel.de; fschott@ifm.uni-kiel.de)

(Received October 24, 1996; revised June 5, 1997; accepted June 11, 1997.)